Dalton Transactions

Accepted Manuscript

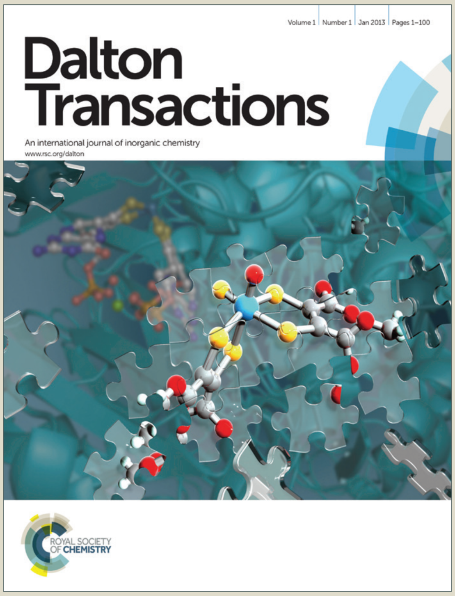

ROYAL SOCIETY OF CHEMISTRY

www.rsc.org/dalton

(Phenoxyimidazolyl-salicylaldimine)iron Complexes: Synthesis, Properties and Iron Catalysed Ethylene Reactions

Margaret Yankey,[a] Collins Obuah,[a] Ilia A. Guzei,[a,b] Emmanuel Osei-Twum,[c] Giovanni Hearne,[d*] and James Darkwa[a*]

[a]*Department of Chemistry, University of Johannesburg, Auckland Park Kingsway Campus, Auckland Park, 2006, South Africa.*

[b]*Department of Chemistry, University of Wisconsin-Madison, 1101 University Avenue, Madison, WI 53706, USA.*

[c]*Saudi Basic Industries Corporation, P.O. Box 42503, Riyadh, 11551, Saudi Arabia.*

[d]*Department of Physics, University of Johannesburg, Auckland Park Kingsway Campus, Auckland Park, 2006, South Africa.*

The reaction of 2-{[2-(1H-imidazol-4-yl)-ethylimino]-methly}-phenol (**L1**), 2,4-di-tert-butyl-6-{[2-(1H-imidazol-4-yl)-ethylimino]-methyl}-phenol (**L2**) or 4-tert-butyl-2-{[2-(1H-imidazol-4-yl)-ethylimino]-methly}-phenol (**L3**) with iron(II) precursors produced either iron(II) or iron(III) complexes, depending on the nature of the anions in the iron(II) precursor and the ligand. When the anion is chloride and the ligand **L1**, the product is $[(\mathbf{L1})_2Fe][FeCl_4]$ (**1**), but when the anion is triflate (OTf^-) and the ligand is **L2**, the product is $[(\mathbf{L2})_2Fe][OTf]_2$ (**2**). With iron(II) halides and *tert*-butyl groups on the phenoxy ligands **L2** and **L3,** the iron(III) complexes $[(\mathbf{L2})FeX_2]$ {where X = Cl (**3**), Br (**4**) and I = (**5**)} and $[(\mathbf{L3})FeCl_2]$ (**6**) were formed.

Complexes **1-6** were characterised by a combination of elemental analyses, IR spectroscopy and mass spectrometry; and in selected cases (**3** and **4**) by single crystal X-ray crystallography. The crystal structures of **3** and **4** indicated that the iron(II) precursors oxidised to iron(III) in forming complexes **3-6**; an observation that was corroborated by the magnetic properties and the ^{57}Fe Mössbauer spectra of **3** and **4**. The iron(III) complexes **3-6** were used as pre-catalysts for the oligomerisation and polymerisation of ethylene. Products of these ethylene reactions depended on the solvent used. In toluene ethylene oligomerised mainly to 1-butene and was followed by the 1-butene alkylating the solvent to form butyl-toluenes *via* a Friedel-Crafts alkylation reaction. In chlorobenzene, ethylene oligomerised mainly to a mixture of C_4-C_{12} alkenes. Interestingly small amounts of butyl-chlorobenzenes and hexyl-chlorobenzenes were also formed *via* a Friedel-Crafts alkylation with butenes and hexenes from the oligomerisation of ethylene.

Introduction

Since the pioneering work by Brookhart and co-workers on α-diimines nickel(II) and palladium(II) complexes as catalysts for the oligomerisation and polymerisation of ethylene and other α-olefins,[1,2] there has been renewed focus on late transition metals as ethylene transformation catalysts as indicated by several reports in this area.[3] Development of iron and cobalt catalysts in particular was sparked by the independent reports[4-6] of Gibson and Brookhart on bis(arylimino)pyridine- iron and cobalt as catalysts for ethylene oligomerisation and polymerisation reactions leading to highly linear products. Depending on the substituents on the bis(arylimino)pyridine ligand, these iron and cobalt complexes are excellent catalysts for ethylene oligomerisation reactions that have high activity and selectivity for making α-olefins, but when polymerisation occurs the products are mainly linear high density polyethylene.[4b,5a,c]

Iron as a metal for producing catalysts is gaining a lot of attention in various organic transformations due to its earth abundance, low toxicity and low cost. With N^N^N bis(arylimino)pyridine ligands, iron(II) form complexes that catalyse ethylene oligomerisation.[7] These (N^N^N)iron(II) catalysts have been modified through variations of substituents on the ligand backbone which have in several instances improved the activity of these catalysts.[8-10] However, unlike the α-diimine nickel and palladium catalysts[11] the active species from bis(arylimino)pyridineiron pre-catalysts are not well understood. EPR and Mössbauer studies have revealed that a bis(arylimino)pyridineiron(II) pre-catalyst gets oxidized to iron(III) species upon activation with MAO as co-catalyst.[12] In fact iron(II) and iron(III) pre-catalysts of the same bis(arylimino)pyridine ligand have been reported to show similar catalytic activities for the production of polyethylene.[5b] This similarity in the activities suggests that the same active species are involved in reactions that use iron(II) and iron(III) pre-catalysts, although the exact nature of these species is unknown.[5b,13] Other reports have shown that bis(arylimino)pyridineiron(III) complexes are good catalysts for the oligomerisation of ethylene to C_4-C_{12} linear α-olefins.[14]

The above narration suggests that imine containing ligands produce excellent catalysts with iron. One such ligand type is salicylaldimine which has been used in making excellent titanium and zirconium ethylene polymerisation catalysts.[15]

However, there are very few salicylaldimine- iron(II) or iron(III)[16] catalysts. The few that are reported are used in atom transfer radical polymerisation (ATRP).[16a] We have, therefore, investigated O^N^N salicylaldimineiron(III) complexes as catalysts for ethylene oligomerisation and polymerisation reactions. The products formed from the ethylene reaction catalysed by these iron(III) catalyst are highly dependent on the solvent in which the reaction is run.

Results and discussion

Synthesis of iron complexes

The reaction of iron(II) chloride with **L1** formed the iron(II) complex [(**L1**)$_2$Fe][FeCl$_4$] (**1**) (Scheme 1), whereas **L2** and **L3** reacted with iron(II) halides to form [(**L2**)FeX$_2$] {where X = Cl (**3**), Br (**4**) and I = (**5**)} and [(**L3**)FeCl$_2$] (**6**) (Scheme 2). A similar iron(II) complex, [(**L2**)$_2$Fe][OTf]$_2$ (**2**) (Figure S1), was formed when the iron(II) precursor was iron(II) trifluoromethanesulfonate. The formation of complexes **3-6** suggested that in forming these complexes intermediate iron(II) complexes are formed, which are oxidised by HX (a by-product) to the iron(III) product (Scheme 2). To test this hypothesis, **L2** was reacted with the iron(II) chloride in the presence of a large excess of Et$_3$N. This led to the isolation of the proposed intermediate [(**L2**)FeCl] (**7**), confirming that all the iron(III) complexes, **3-6**, were formed *via* the intermediate in Scheme 2. The acidic phenolic-OH was deprotonated by the Et$_3$N and formed an ammonium salt with the chloride, thereby preventing any oxidation of the iron(II) to iron(III) by HCl formed from the deprotonation of the phenolic proton. Gibson and co-workers have prepared similar iron(II) complexes as catalysts in ATRP.[16a] Reacting iron(III) chloride with **L2** under the same reaction conditions used to prepare **3** gave a compound that analysed exactly as complex **3** (Figure S2)

Complexes **2**, **4**, **5** and **7** were purified by recrystallisation from toluene and hexane, while **1**, **3** and **6** were purified by recrystallisation from dichloromethane and hexane. All the products were isolated in moderate to high yields (44-73%) as dark blue solids except complexes **5** and **7** which were isolated as dark green solids.

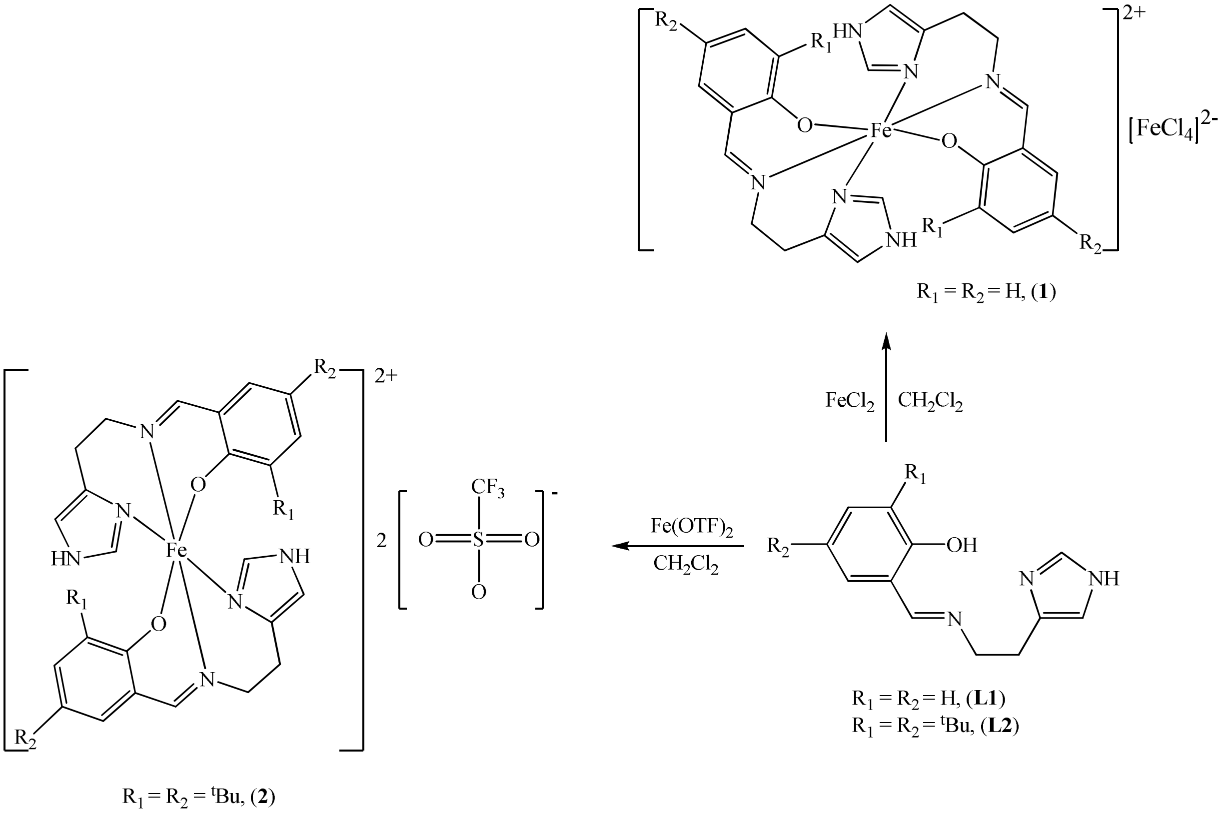

Scheme 1: Synthesis of bis(O^N^N salicylaldimine)iron(II) complexes

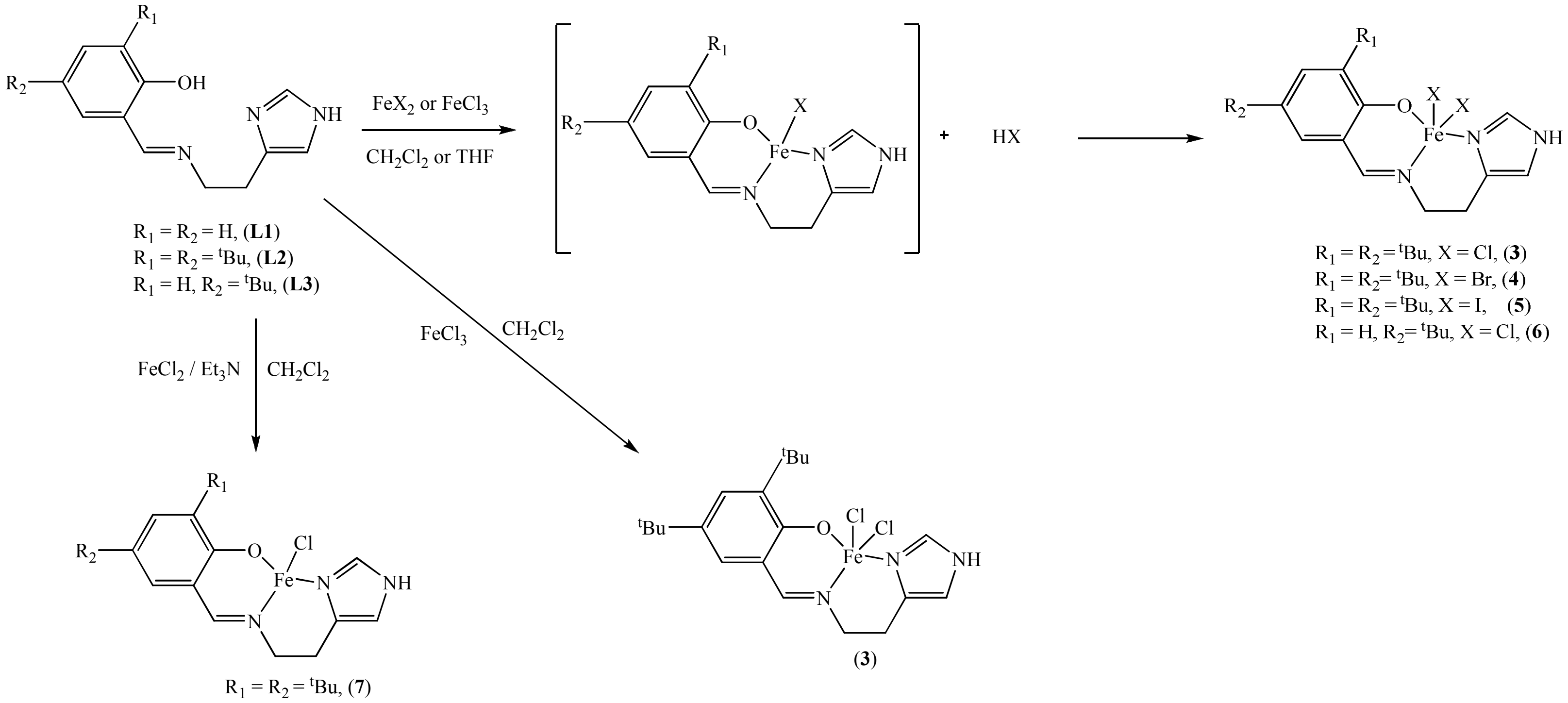

Scheme 2: Synthesis of O^N^N salicylaldimineiron(III) complexes from iron(II) precursors

The infrared spectra of the complexes showed υ(C=N) peaks in the range of 1599-1619 cm^{-1} (Figures S3-S9) which are lower and weaker in intensity compared to the peaks in the ligands in the range 1630-1631 cm^{-1}. These observations support the presence of imine groups in the iron complexes and also the binding of the ligands to the iron centres.[17] The nature of complexes **3-6** was first established from the single crystal X-ray structures of **3** and **4** as iron(III) halide complexes (Figures 1 and 2). Microanalyses were subsequently used to confirm that these complexes indeed have two halides bound to the iron metal centre and were pure. These observations, therefore, are enough evidence that **3-6** were formed *via* the oxidation of iron(II) intermediates by *in situ* formed HX (X = Cl, Br or I). Similar formation of nickel(III)[18] complexes from nickel(II) by strong acids have been reported in literature.

The formation of complex **2** is the result of the inability of triflic acid, the expected by-product from this reaction, to oxidise the intermediate in Scheme 1. A molecular structure of complex **2** (Figure S1) was obtained but with a high R factor. As such the bond lengths and angles are not discussed. The molecular structure however confirmed the connectivity of the salicylaldimine ligand **L2** to the iron(II) precursor bearing weak counterion. This salt consists of two cationic molecules of **L2** with two triflate ions as counterions. The iron metal centre is coordinated through the donor oxygen atoms, imine-N atoms and imidazolyl-N atoms. On the other hand the lack of steric bulk for **L1** leads to the formation of complex **1**. In fact the tri-dentate 2,6-bis(1-phenylimino)ethyl)pyridine ligand, without substituents on the iminophenyl ring, is reported to form an ionic compound comprising of [(**L**)$_2$Fe] and [$FeCl_4$] ions (L = 2,6-bis(1-phenylimino)ethyl)pyridine).[19] Similar ion-pair iron(II) complexes have been described for various bis(arylimino)pyridine compounds.[14b,c,20] Mass spectrometry was used in the characterization of both **1** and **2**. For instance with **1**, negative ion high resolution electrospray ionization mass spectrometry identified the anion as $[FeCl_4]^{2-}$ (m/z = 195.8104) while the corresponding cation was identified by positive ion high resolution electrospray ionization mass spectrometry as $[Fe(\mathbf{L3})_2]^{2+}$ (m/z = 484.1312) (Figure S10).

Molecular structures of 3 and 4

Dark blue single crystals of complexes **3** and **4** suitable for the X-ray structural determination were obtained by slow evaporation of toluene and hexane solutions of these complexes at room temperature. Crystallographic data are provided in Table 1, whereas Figure 1 and Figure 2 show the molecular structures of these compounds. Central metals in complexes **3** and **4** are pentacoordinate and have a distorted geometry about the metal centre consistent with a complex nature of metal-ligand binding. According to the criterion τ developed by Addison *et al.*[21] the structure is square pyramidal when $\tau = 0$ and trigonal pyramidal when $\tau = 1$. For compounds **3** and **4** the values of τ are 0.56 and 0.52, indicating a transitional conformation between the two idealized geometries.

Complex **3** has been obtained by two synthetic routes (Scheme 2). This indicates that starting from either iron(II) or iron(III) metal source results in the formation of the same iron(III) complex for this ligand **L2**, thus confirming that iron(II) starting precursors are indeed oxidised to iron(III) products. In **3**, one of the chlorides, Cl1, occupies the apical position of the square pyramid with the Fe-Cl bond lengths noticeably unequal. That is the bond to the apical chloride is significantly longer (2.316(7) Å) than that of its basal counterpart (2.277(7) Å). The Fe-N($_{imino}$) distance in **3** (2.130(2) Å) is longer than the Fe-N($_{imidazole}$) **3** (2.094(2) Å) probably as a consequence of satisfying the tri-dentate chelating constraints of the ligand as described by Gibson *et al.* for diimine iron complexes.[5a] The fifth bond, Fe1-O1 (1.860(17) Å) falls in the usual range. The bond angles around the iron(III) centre O1-Fe1-N$_{imino}$, 85.44(7)°, N1-Fe1-N$_{imino}$ 85.63(7)°, O1-Fe1-Cl1, 91.25(5)° and N$_{imidazole}$-Fe1-Cl1, 91.07(6)° show deviations from the expected 90° angles for a square pyramidal geometry.

In complex **4** the Fe-N$_{imino}$ bond length (2.126(2) Å) is similarly longer than the Fe-N$_{imidazole}$ (2.095(3) Å) and Fe-O1 (1.851(2) Å) bond length compares well to that in **3**. It is also interesting to note that there is no significant effect on the imine bond length in the coordinated ligands in either complex (i.e. N3-C6 in **3** and N1-C7 in **4** measure 1.289(3) Å and 1.286(4) Å respectively and are typical of the HC=N bond).[22]

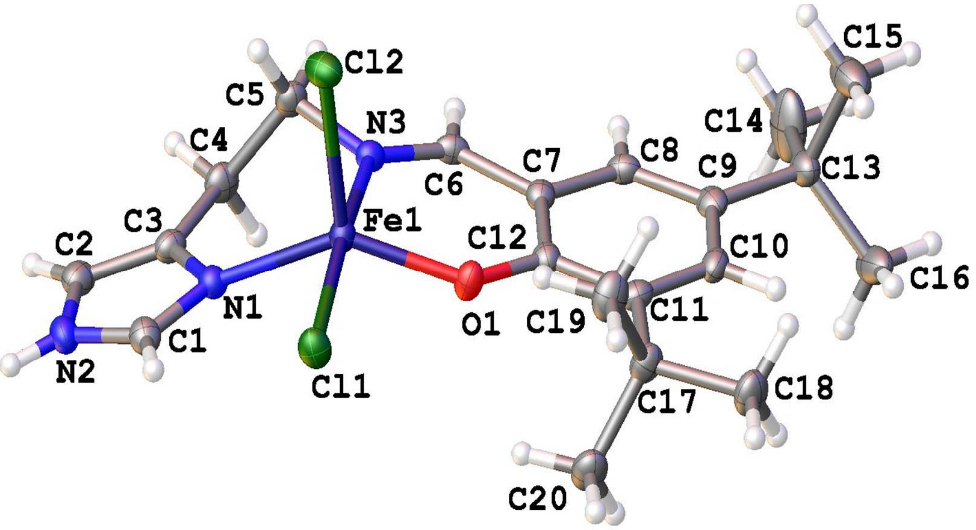

Figure 1: Molecular structure of **3** with the 50% probability ellipsoids. Selected bond lengths (Å) and angles (°) are: Fe1-O1, 1.860(17); Fe1-N1, 2.094(2); Fe1-N3, 2.130(2); Fe1-Cl1, 2.277(7); Fe1-Cl2, 2.316(7); O1-C12, 1.324(3); N3-C6, 1.289(3); O1-Fe1-N1, 137.16(8); O1-Fe1-N3, 85.44(7); N1-Fe1-N3, 85.63(7); O1-Fe1-Cl2, 113.02(6); N1-Fe1-Cl2, 108.85(6); N3-Fe1-Cl2, 90.30(6); O1-Fe1-Cl(1), 91.25(5); N1-Fe1-Cl1, 91.07(6); N3-Fe1-Cl1 170.86(6); Cl2-Fe1-Cl1, 98.84(3); C5-N3-C6, 116.0(2).

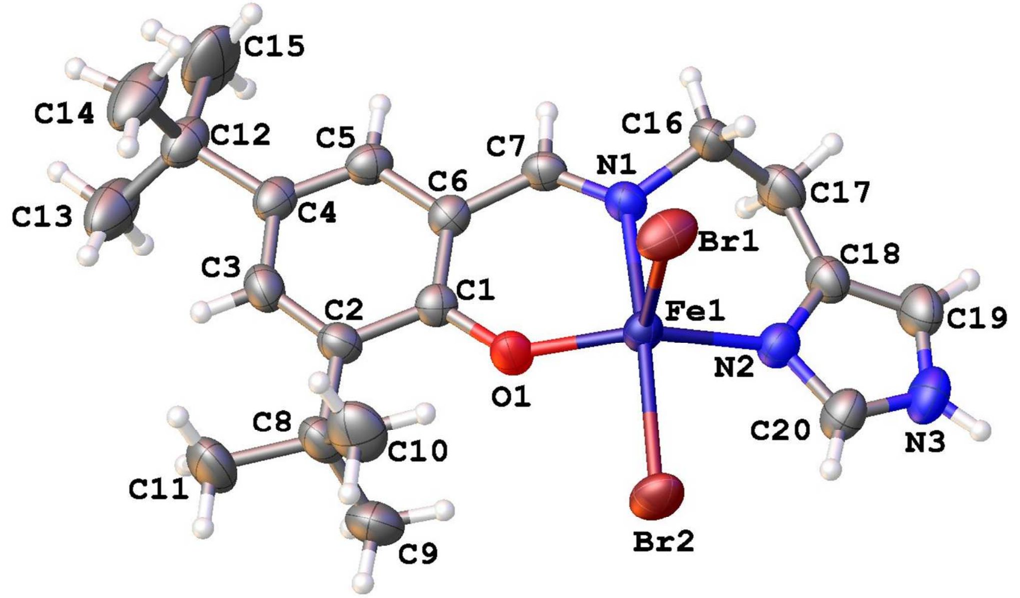

Figure 2: Molecular structure of **4** with the 50% probability ellipsoids. Selected bond lengths (Å) and angles (°) are: Fe1-O1, 1.851(2); Fe1-N1, 2.126(2); Fe1-N2, 2.095(3); Fe1-Br2, 2.471(7); Fe1-Br1, 2.415(7); O(1)-C(1), 1.319(3); N1-C7, 1.286(4); O1-Fe1-N1, 85.49(9); O1-Fe1-N2, 138.96(10); N1-Fe1-N2, 85.54(9); O1-Fe1-Br2, 90.20(6); N1-Fe1-Br2, 169.90(7); N2-Fe1-Br2, 91.78(7); O1-Fe1-Br1, 112.10(8); N1-Fe1-Br1, 90.98(7); N2-Fe1-Br1, 108.01(7); Br2-Fe1-Br1, 99.11(3); C7-N1-C16, 116.2(2).

Table 1: Crystal data collection and structural refinement parameters for **3** and **4**

Parameters	**3**	**4**
Empirical formula	$C_{20}H_{28}Cl_2FeN_3O$	$C_{20}H_{28}Br_2FeN_3O$
Formula weight	453.2	542.12
Temperature/K	100(1)	296(2)
Wavelength/Å	1.54178	0.71073
Crystal system	Orthorhombic	Orthorhombic
Space group	$P2_12_12_1$	$P2_12_12_1$
a/ Å	7.7909(3)	7.931(2)
b/Å	14.1052(5)	14.457(4)
c/Å	19.9130(7)	20.040(7)
α/°	90	90
b/°	90	90
g/°	90	90
Volume/$Å^3$	2188.28(14)	2297.8(12)
Z	4	4
Density (calculated)/Mg/m^3	1.376	1.567
Absorption coefficient/mm^{-1}	7.882	4.148
F(000)	948	1092
Goodness-of-fit on F^2	1.038	1.049
Final R indices [I>2sigma(I)]	R1 = 0.0294, wR2 = 0.0685	R1 = 0.0247, wR2 = 0.0617
R indices (all data)	R1 = 0.0335, wR2 = 0.0702	R1 = 0.0273, wR2 = 0.0629

Magnetic behaviour and ^{57}Fe Mössbauer effect spectroscopy (MES) of iron(III) complexes 3 and 4

To further investigate the spin state of the iron(III) complexes **3** and **4**, variable-temperature magnetic susceptibility measurements were conducted on powder samples of **3** and **4** in the temperature range 2-300 K on a SQUID magnetometer. The susceptibility values were calculated in cgs units. The data are presented as $\chi_M.T$ versus T plots. The $\chi_M.T$ value for **3** at 300 K is 4.35 cm^{-3}.mol^{-1}.K (Figure 3) corresponding to a μ_{eff} of 5.90 BM. This value is consistent with HS iron(III).[16b,23] At high temperatures up to 300 K, μ_{eff} is temperature-independent (Figure 4 inset). As the temperature is lowered from 300 K, $\chi_M.T$ remains constant until approximately 50 K then decreases sharply to $\chi_M.T$ = 2.25 cm^{-3}.mol^{-1}.K at 2 K. No maximum of the susceptibility is observed in the temperature range studied. The sharp drop at low temperatures is likely due to a zero-field splitting (spin-orbit coupling effect) and or very weak intermolecular magnetic interactions.[24] The former is likely, as this is expected to be dominant at low temperatures, taking into account the mononuclear nature of the complex and the anticipated absence of intermolecular iron-iron interactions.

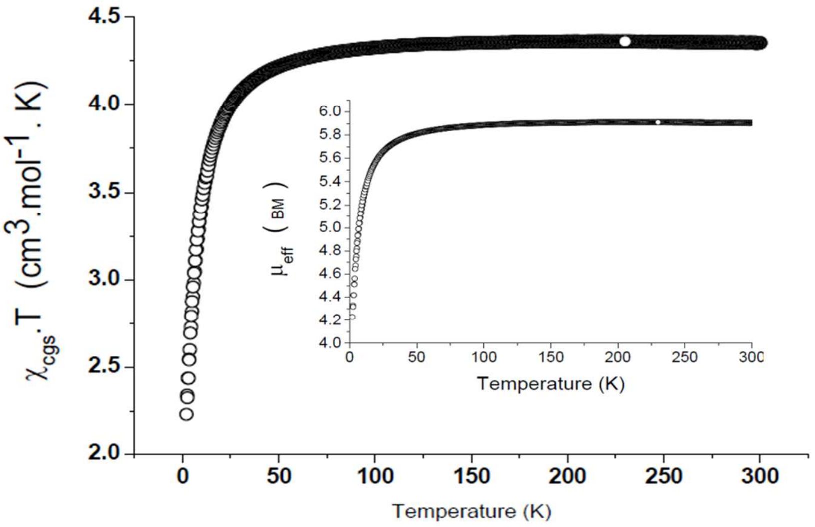

Figure 3: $\chi_M.T$ product versus T plot for **3** (inset = μ_{eff} versus T plot).

At the lowest temperature of measurement (2 K) the $\chi_M.T$ value is 2.25 cm^{-3}.mol^{-1}.K which corresponds to μ_{eff} of 4.22 BM. The value is lower than that for HS and higher than that for LS. It is however in the range of $\chi_M.T$ (1.8-2.8 cm^{-3}.mol^{-1}.K) and μ_{eff} (3.9-4.5 BM) for IS iron(III) (S = 3/2) with 3 unpaired electrons.[24] ^{57}Fe Mössbauer spectroscopy at liquid helium temperatures would be necessary to confirm this. The spin pairing would lead to a large increase in quadrupole splitting, E_Q, parameter in comparison to the HS electronic scenario.[25] Plot of $1/\chi_{cgs}$ against temperature (Figure 4) shows expected linearity typical of paramagnetic behaviour. It however does not extrapolate to zero obeying the Curie Weis law with a negative Weiss temperature. The hint of a downturn at low temperatures as well as this negative Weiss temperature is typical of ferrimagnetic behaviour. It is interesting that such a hint of ferrimagnetism occurs in a metal complex having only a single transition-metal component. All of the reported compounds that exhibit ferromagnetic behaviour include at least two magnetic components: bimetallic complexes or metal complexes with organic radicals.[26]

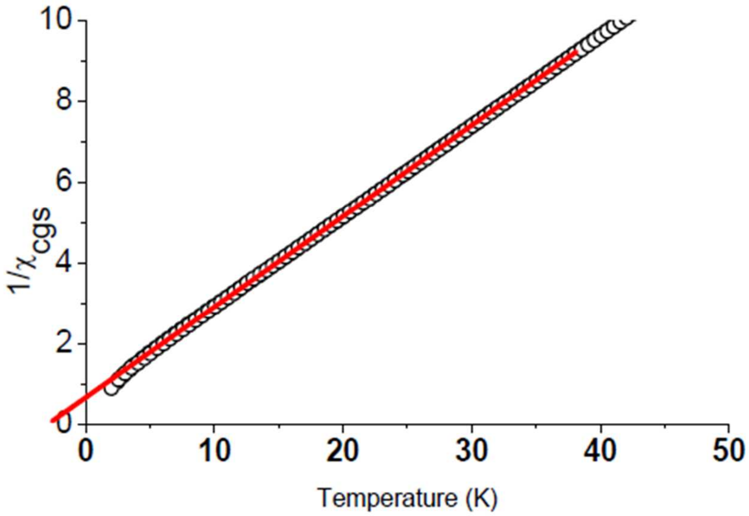

Figure 4: $1/\chi_{cgs}$ versus *T* plot for **3** showing a hint of ferrimagnetic behaviour.

For complex **4**, the $\chi_M.T$ at high temperature (300 K) is 4.54 $cm^{-3}.mol^{-1}.K$ and 0.70 $cm^{-3}.mol^{-1}.K$ at low temperature of 2 K. These values correspond to a μ_{eff} of 6.02 (HS) and 2.4 (LS) BM respectively, which are a little higher than the anticipated spin-only values for both HS and LS iron(III) complexes. Nonetheless, they are typical values observed for other similar HS and LS iron(III) complexes of this kind.[27] In Figure 5, the $\chi_M.T$ is constant at high temperatures from 300 K until approximately 50 K when it drops rapidly till 2 K. A broad maximum is observed in the range of 6-13 K and then the susceptibility decreases slowly until 100 K (Figure 5 inset). The plot of $1/\chi_{cgs}$ against T does not extrapolate to zero as well indicative of some degree of antiferromagnetic behaviour (Figure 6).

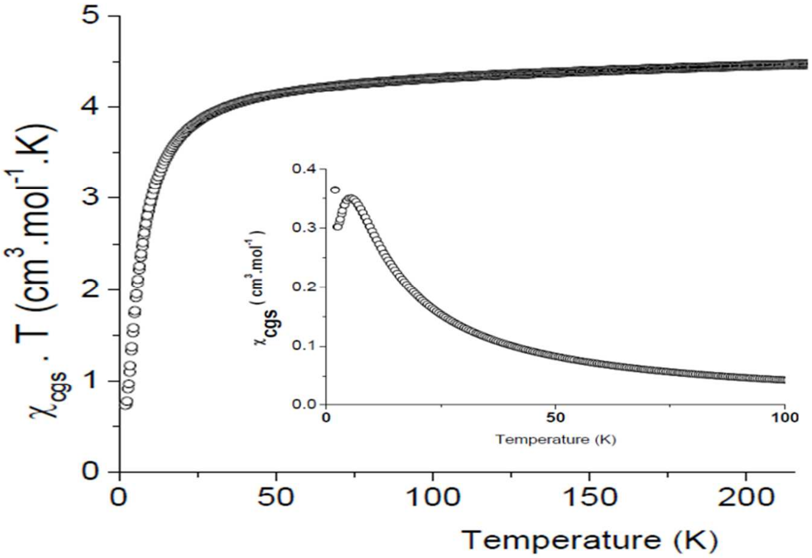

Figure 5: $\chi_M.T$ product versus T plot for **4** with the low-T region of the temperature dependent molar susceptibility expanded as inset.

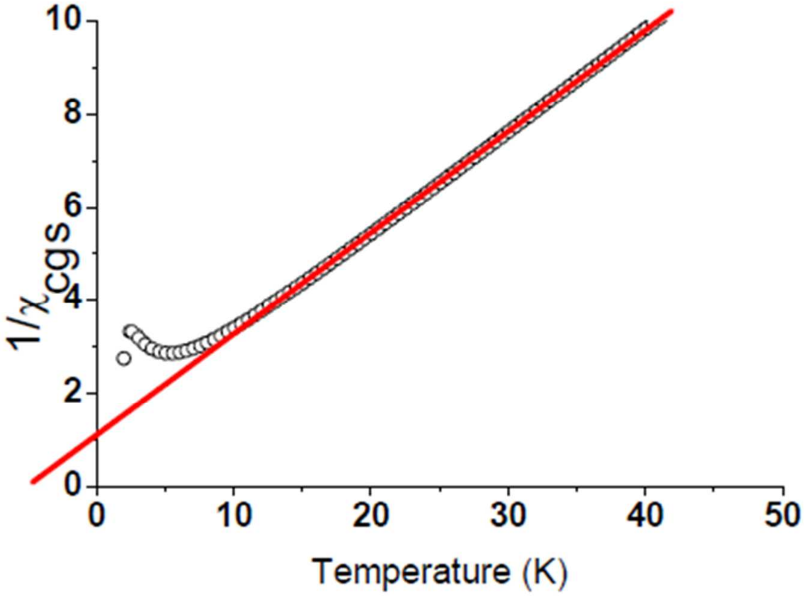

Figure 6: $1/\chi_{cgs}$ versus *T* plot for **4** showing antiferromagnetic behaviour.

Mössbauer spectroscopy was used as a further tool to investigate the spin state of the iron(III) in complexes **3** and **4**. The Mössbauer data for both complexes **3** and **4** (*vide infra*) show only a single doublet at both 300 K and 157 K. The quadrupole splitting (E_Q) calculated for both complexes are consistent with E_Q values (0.6-1.3 mm.s^{-1}) for HS iron(III). It is therefore evident that at these temperatures only the HS state is observed corroborating the magnetic susceptibility data. As is characteristic of transition-metal complexes displaying spin-transition behaviour, the higher spin state is favoured at high temperatures while the spin paired (IS or LS) state is favoured at low temperatures. Mössbauer measurements were also taken at 15 K. This was on a sample that had been in storage for several months. Some degradation was evident in the spectrum that was re-measured at room temperature. The measured E_Q values of the sub-component in this sample do not increase substantially upon cooling to 15 K and are in the order of ≈1.4 mm.s^{-1}. A spin state transition would involve a much bigger increase compared to the high temperature (HS) value, E_Q ≈1.1 mm.s^{-1}. Based on the susceptibility results shown in Figure 6, the precipitous decrease in μ_{eff} is ascribed to antiferromagnetic coupling of molecular units.

The ^{57}Fe Mössbauer spectra of complexes **3** and **4** provide further evidence that these iron complexes are in the +3 oxidation states. ^{57}Fe Mössbauer spectra were measured for complexes **3** and **4** at 300 K and after fitting the spectra we observed the spectra were asymmetric doublets with isomer shifts of δ = of 0.36 mm.s^{-1} for **3** and 0.38 mm.s^{-1} for **4** (Table 2). These isomer shifts are consistent with high spin iron(III) ions in an N^O coordination environment (where IS ≈ 0.35 mm.s^{-1}).[28] The asymmetry in the intensities of ^{57}Fe Mössbauer spectra (doublets) can be attributed to spin-spin relaxation effects. The ^{57}Fe Mössbauer spectra for **3** and **4** were also measured at 157 K (Figure S11). The degree of asymmetry decreased with decreasing temperature as reported in the literature.[29] We also observed a change in isomer shift $\Delta\delta$ = 0.08 mm.s^{-1} for both complexes due to the second-order Doppler Effect.[30] Quadrupole splitting (E_Q) values are weakly temperature dependent, are relatively small and this also corroborates the high spin nature of the iron(III) complexes. The quadrupole splitting values in **4** are systematically higher than in **3** (Table 2). The difference in the quadrupole splitting between complexes **3** and **4** can be explained by the different halides on the iron(III) metal centre. This influences the electric field gradient at the iron(III) nucleus, hence the difference.

Table 2: ^{57}Fe Mössbauer parameters obtained at variable temperatures, ^{a}300 K and ^{b}157 K

Complex	δ (mm.s^{-1})	E_Q (mm.s^{-1})
3^{a}	0.36	1.15
4^{a}	0.38	1.19
3^{b}	0.44	1.27
4^{b}	0.46	1.32

Catalysis

Ethylene oligomerisation and polymerisation using complexes 3-6

The iron(III) complexes **3-6** produced active catalysts upon activation with $EtAlCl_2$ for the oligomerisation and polymerisation of ethylene. The generation of the active catalysts was highly exothermic, with reactor temperatures immediately reaching 50-80 °C upon activation with the co-catalyst. The temperatures, however, dropped for the remainder of the reaction time to 25 °C. Similar exothermic processes have been reported for other transition metal catalysed ethylene oligomerisation reactions.[31]

All four complexes catalysed the oligomerisation and polymerisation of ethylene and exhibited high catalytic activities for these reactions ($0.30\text{-}9.55 \times 10^{6}$ g.molFe^{-1}.h^{-1}) (Table 3). The activities obtained are comparable with those of similar iron(II) (13.9×10^{6} g.molFe^{-1}.h^{-1})[17a] and iron(III) (2.16×10^{5} g.molFe^{-1}.h^{-1})[32]

catalysts. Most iron complexes that have been reported in literature produce both ethylene oligomers and polymer (waxes) but with MAO as the co-catalyst.[17a,33] In the case of the O^N^N salicylaldimineiron(III) pre-catalysts used in this work, the type of oligomers and polymers produced were solvent dependent. The effect of solvent on the catalytic activity and the products obtained was thus investigated in detail with pre-catalyst **3**.

Effect of solvent on the catalytic activity and products formed

Using toluene as the solvent, three types of products were obtained: 1-butene, C_2 and C_4 alkyl-toluenes and polyethylene. The C_2 and C_4 alkyl-toluenes were identified and characterised by GC (Figure S12) and GC-MS (Figure S13 and S14). So the formation of 1-butene is inferred from the formation of butyl-toluenes. It is believed that the reaction between the pre-catalyst **3** and $EtAlCl_2$ produced a tandem catalyst that catalysed ethylene to 1-butene and *via* Friedel-Crafts alkylation gave ethyl- and butyl- *o*-/*p*-C_6H_5. Such alkylation products have been reported by Darkwa and co-workers using nickel(II) (pyrazol-1-ylmethyl)pyridine,[34] (3,5-dimethylpyrazol-1-yl)methylbenzene[35] pyrazolylpyridylamine and pyrazolylpyrroleamine[36] catalysts. The ethylene reaction also produced a small amount of polyethylene (0.39 g; entry 5, Table 3). The polymer was characterized by $^{13}C\{^1H\}$ NMR spectroscopy (Figure S14) and GPC, which showed unimodal molecular weight distribution (Figure S16) with $M_w = 60.4 \times 10^3$ g.mol^{-1} and M_w/M_n of 2.2. This GPC data confirms the single-site nature of the iron catalysts.

Table 3: Oligomerisation and polymerisation of ethylene with **3-6**/$EtAlCl_2$[a]

Entry	Pre-catalyst	Product distribution (%)[b]						α	Activity[c] × 10^6	Oligomer Yield (g)	Polymer Yield (g)	m/z[d]
		C_4	C_6	C_8	C_{10}	C_{12}	F-C					
1	**3**	35	30	12	12	7	4	0.58	9.55	98.35	6.65	758.22
2	**4**	43	38	10	6	2	1	0.33	2.00	17.33	4.67	850.26
3	**5**	49	39	5	3	2	2	0.67	2.55	24.65	3.35	809.67
4	**6**	28	21	16	15	14	6	0.90	3.64	36.59	3.41	833.24
5	**3**[e]	-	-	-	-	-	100	-	0.79	8.28	0.39	60.40[f]

[a]Reaction conditions: Chlorobenzene (70 mL), Al:Fe (400), reaction temperature (30 °C), reaction time (1 h) and ethylene pressure (10 bar). [b]Determined by GC. [c]Activity = $g.molFe^{-1}.h^{-1}$). [d]ESI-MS of polymer. [e]Toluene (70 mL). [f]Determined by GPC, × 10^3 $g.mol^{-1}$. α = Schulz-Flory coefficient.

Using chlorobenzene as solvent gave three types of products. The first type of product was a mixture of C_4-C_{12} (Figure S17) ethylene oligomers that followed a Schulz-Flory distribution, with α coefficient in the range of 0.33-0.93. The major component of the product ethylene oligomers were butenes and hexenes, but at high Schulz-Flory coefficients there was higher decene and dodecene components in the mixture (Table 3).[37] The second type of products were oils with carbon content > C_{30}). Typical ^1H (Figure S18) and $^{13}C\{^1H\}$ NMR spectroscopic data (Figure 7) showed these are highly branched olefins.[38] Their ESI-MS data showed these oils have low molecular weights (Table 3), suggesting that they are oligomers with high carbon content and not polymers. The third type of products is small amounts of alkyl-chlorobenzenes in the product mixture. These alkyl-chlorobenzenes were characterised by GC (Figure S17) and GC-MS (Figures S19, S20 and S21) and identified as mono- and di- butyl-chlorobenzenes and mono-hexyl-chlorobenzene which were formed *via* Friedel-Crafts alkylation of chlorobenzene by butenes and hexenes from the oligomerisation of ethylene. Although Friedel-Crafts alkylation of deactivated aromatic solvents such as chlorobenzene is less likely compared to alkylation of activated aromatic solvents such as toluene, there have been reports of halo-benzenes that have been alkylated with polychlorinated methanes.[39] To the best of our knowledge, there is no report on Friedel-Crafts alkylation of halo-benzenes with alkenes.

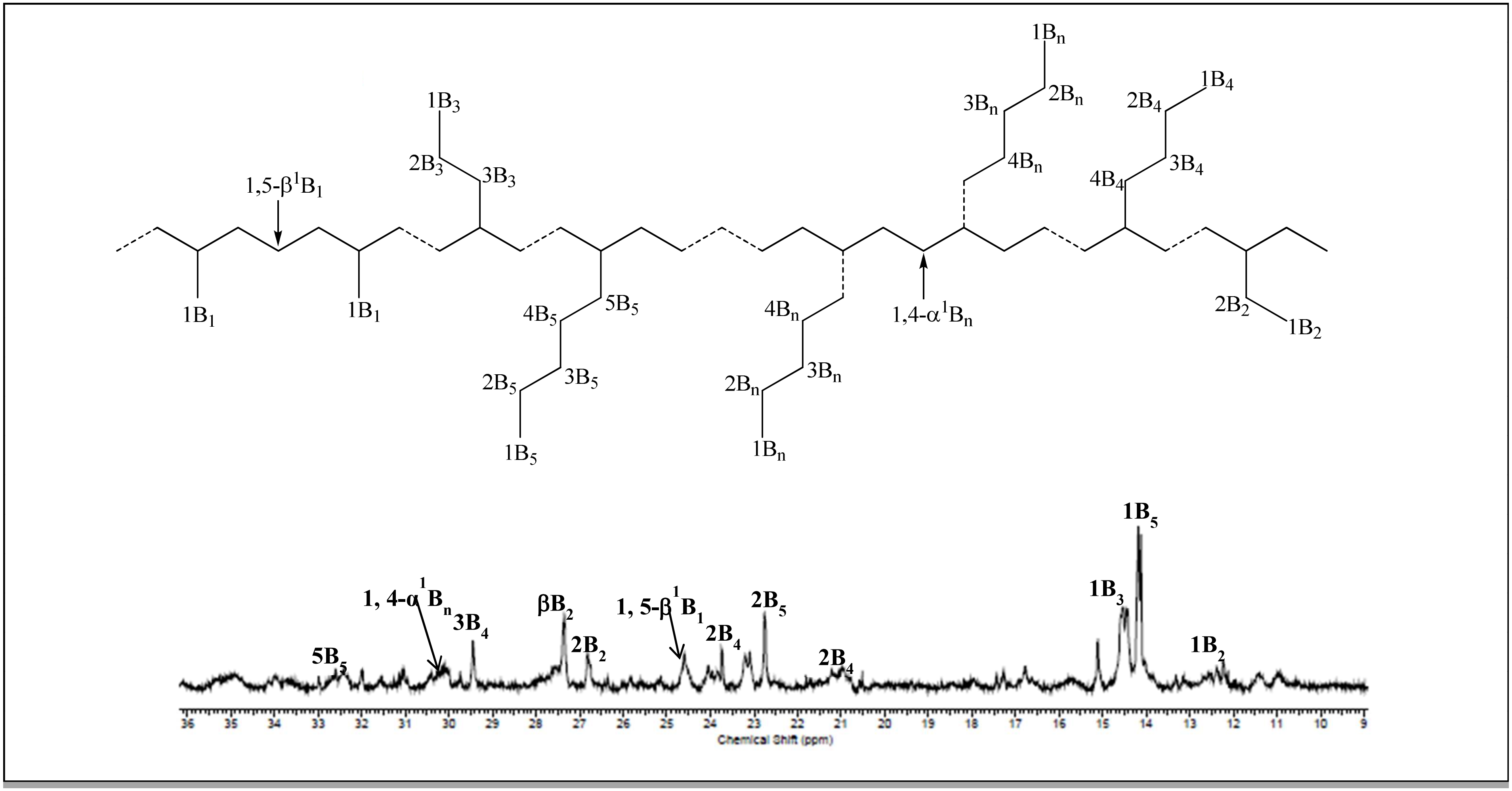

Figure 7: Typical ^{13}C {^{1}H} NMR spectrum of oils obtained using **3**/EtAlCl$_2$

Effect of reaction parameters on catalytic activity of 3/$EtAlCl_2$

The pre-catalyst **3** with $EtAlCl_2$ was used to investigate the effect of reaction parameters such as ethylene pressure, Al:Fe ratio and reaction time. The data obtained from these variations is summarized in Table 4. Kinetic studies have shown that increasing the pressure of ethylene increases the rate of oligomerisation.[40] Therefore ethylene oligomerisation reactions were performed at varying ethylene pressures (entries 3, 6, 7 and 8, Table 4). At ethylene pressure of 5 bar, catalyst activity was 2.55×10^6 $g.molFe^{-1}.h^{-1}$ (entry 6, Table 4), which increased as the pressure was increased to 10 bar ($0.61\text{-}9.55 \times 10^6$ $g.molFe^{-1}.h^{-1}$, entry 3, Table 4). However, the catalyst activity decreased with increasing pressure at 15 bar ($0.07\text{-}7.00 \times 10^6$ $g.molFe^{-1}.h^{-1}$, entry 7, Table 4) and 20 bar ($0.05\text{-}5.27 \times 10^6$ $g.molFe^{-1}.h^{-1}$, entry 8, Table 4). The reduction in activity as pressure reached 15 bar could be due to saturation of ethylene in the reaction mixture.[41]

The amount of co-catalyst used was also found to have substantial effect on catalyst activity. Catalytic activity increased when the Al:Fe ratio was increased from 300:1 to 400:1, but activity decreased when Al:Fe ratio was further increased beyond 400:1 (entries 1-3, Table 4). The highest oligomerisation activity (9.55×10^6 $g.molFe^{-1}.h^{-1}$) was obtained with Al:Fe ratio of 400:1 and ethylene pressure of 10 bar (entry 3, Table 4). Reaction time was also varied from 30 to 180 min (entries 3, 9-11, Table 4) leading to optimum activity at 60 min but activity decreased as reaction time was increased to 180 min. This decrease in activity is indicative of catalyst deactivation with reaction time.

Table 4: Ethylene oligomerisation and polymerisation data using **3**/$EtAlCl_2$[a]

Entry	Al:Fe	Pressure (bar)	Time (min)	Product distribution (%)[b]						α	Activity[c] × 10^6	Oligomer Yield (g)	Polymer Yield (g)	m/z[d]
				C_4	C_6	C_8	C_{10}	C_{12}	F-C					
1	300	10	60	44	34	8	6	2	6	0.33	4.00	39.52	4.48	708.38
2	350	10	60	42	32	11	7	4	4	0.57	5.00	50.22	4.78	743.66
3	400	10	60	35	30	12	12	7	4	0.58	9.55	98.35	6.65	758.22
4	450	10	60	36	33	12	10	7	2	0.70	5.55	53.79	7.21	998.29
5	500	10	60	26	33	15	12	9	5	0.75	4.55	42.08	7.92	673.58
6	400	5	60	44	35	8	7	4	2	0.57	2.55	28.00	-	-
7	400	15	60	64	26	6	3	1	1	0.33	7.00	76.28	0.72	-
8	400	20	60	28	26	24	14	13	5	0.93	5.27	57.44	0.56	1072.29
9	400	10	30	42	35	9	6	5	3	0.83	5.09	21.46	6.54	-
10	400	10	120	59	34	5	2	1	-	0.50	3.77	76.01	6.99	924.29
11	400	10	180	41	29	14	9	7	3	0.78	1.67	48.73	6.27	758.23

[a] Reaction conditions: Chlorobenzene (70 mL), pre-catalyst **3** loading (11 μmol), reaction temperature 30 °C. [b] Determined by GC. [c] Activity = $g.molFe^{-1}.h^{-1}$. [d] ESI-MS of polymer. α = Schulz-Flory coefficient.

Conclusions

Ligand dependent reactions of (imidazol-4-yl)-ethylimino]-methly}phenol ligands with iron(II) halide precursors gave two types of products, namely bis{(imidazol-4-yl)-ethylimino]-methlyphenoxy}iron(II) and O^N^N {(imidazol-4-yl)-ethylimino]-methlyphenoxy}iron(III) halides. The formation of the iron(III) complexes is driven by the oxidation of iron(II) intermediates by HX (X= Cl, Br, I) by-products. These iron(III) complexes can be activated with $EtAlCl_2$ to produce catalysts for ethylene reactions that produce oligomers or polymers depending on the solvent used. In toluene and chlorobenzene alkyl-aromatics *via* Friedel-Crafts alkylation of the solvent with ethylene, butene and hexene lead to ethyl-, butyl- and hexyl-toluenes or chlorobenzenes.

Experimental

Materials and instrumentation

All procedures were performed under dry Argon using standard Schlenk techniques. All solvents were of analytical grade and were dried and distilled under nitrogen prior to use. Ethylene (99.9%) was purchased from AFROX (South Africa) and used as received. The co-catalyst ethylaluminium dichloride ($EtAlCl_2$), 1.0M in hexane was purchased from Sigma-Aldrich and used as received. The O^N^N ligands, 2-{[2-(1H-imidazol-4-yl)-ethylimino]-methly}-phenol (**L1**),[42] 2,4-di-tert-butyl-6-{[2-(1H-imidazol-4-yl)-ethylimino]-methyl}-phenol (**L2**)[43] and 4-tert-butyl-

2-{[2-(1H-imidazol-4-yl)-ethylimino]-methly}-phenol (**L3**)[43] were synthesised according to literature procedures.

The nuclear magnetic resonance (NMR) spectra were recorded on a Bruker 400 MHz instrument (^{1}H at 400 MHz and $^{13}C\{^{1}H\}$ at 100 MHz) at room temperature. Chemical shifts are reported in δ (ppm) and referenced to the residual proton and (7.24 and 77.0 ppm for $CDCl_3$ and 132.36 for *o*-dichlorobenzene-d_4). Infrared (IR) spectra were recorded on a Bruker Tensor 27 equipped with a diamond ATR. Elemental analyses were performed on a Vario Elementar III microcube CHNS analyser. Mass spectra were recorded on a Waters API Quattro Micro spectrophotometer. Variable-temperature (2-300 K) magnetic susceptibility measurements were carried out on a Quantum Design MPMS-5S SQUID magnetometer operating at a magnetic field of 0.5 T with $HgCo(NCS)_4$ as the calibrant. Diamagnetic corrections were performed in the usual way using Pascal's constants. Variable-temperature Mössbauer spectra were recorded on a conventional spectrometer equipped with a Janis cryostat, using a Lakeshore temperature controlling device and a calibrated silicon diode thermometer. $^{57}Co(Rh)$ was used as the source of radiation.

The crystal evaluation and data collection were performed on a Bruker SMART APEXII diffractometer with either Cu K_α (λ = 1.54178 Å) or Mo K_α (λ = 0.71073 Å) radiation and the diffractometer to crystal distance of 4.03 cm or 4.96 cm respectively. The initial cell constants were obtained from three series of ω scans at different starting angles. The reflections were successfully indexed by an automated indexing routine built in the APEXII program. The absorption correction was based on fitting a function to the empirical transmission surface as sampled by multiple equivalent measurements.[44] The structures were solved by direct methods and refined by least squares techniques using OLEX2: a complete structure solution, refinement and analysis program.[45] All non-hydrogen atoms were refined with anisotropic displacement coefficients. All hydrogen atoms were included in the structure factor calculation at idealized positions and were allowed to ride on the neighbouring atoms with relative isotropic displacement coefficients. The refined structure was subjected to the checkCIF criteria of the International Union of Crystallography (IUCr) and no major alerts came up.

General procedure for ethylene oligomerisation and polymerisation reactions

The oligomerisation was carried out in a 450 mL high pressure reactor which was preheated for 1 h at 120 °C under vacuum and cooled under nitrogen to the desired temperature before use. To an appropriate amount of pre-catalyst in a Schlenk tube was added degassed toluene (35 mL) and the solution transferred into the reactor by a cannula. The reactor was then charged with ethylene (3 bar) for 5 min. In a second Schlenk tube containing degassed toluene (35 mL), an appropriate amount of ethylaluminium dichloride (Al:Fe = 300:1-500:1) was added with a syringe. The solution was then transferred via a cannula into the reactor. Immediately after the addition of the $EtAlCl_2$ solution, the reactor was charged with ethylene while the reactor temperature was maintained at the desired temperature. An appropriate amount of ethylene was continuously supplied to maintain a constant pressure in the reactor during the polymerisation reaction. After the set reaction time, excess ethylene was vented and the reaction mixture quenched by adding 2 M HCl solution. The product was sampled for gas-chromatography (GC) analysis.

Synthesis of salicylaldimine iron complexes

A solution of [FeX_2], (X = Cl, Br, I or OTF), in either dichloromethane (complexes **1**, **3**, **4**, **6**, and **7**) or tetrahydrofuran (complex **5**) was added to a solution of the ligand in either dichloromethane or tetrahydrofuran. The resulting blue, green or maroon solution was stirred for 18 h. The solvent was evaporated after the reaction time and the pure product recrystallised from a solution of either dichloromethane and hexane (complexes **1**, **3** and **6**) or toluene and hexane (complexes **2**, **4**, **5** and **7**). All the complexes were synthesised in moderate to good yields.

Synthesis of [bis(2-{[2-(1H-imidazol-4-yl)-ethylimino]-methly}-phenol)iron(II)] [iron(II)tetrachloride] (1): Complex **1** was synthesized using **L1** (0.18 g, 0.84 mmol) and [$FeCl_2$] (0.11 g, 0.84 mmol) as dark blue powder. Yield: 0.25 g, (44%). Anal. Calc. for $C_{24}H_{24}Fe_2Cl_4N_6O_2.1.25CH_2Cl_2.2C_6H_{14}$: C, 46.58; H, 5.72; N, 8.75%. Found: C, 46.47; H, 5.45; N, 9.13%. MS (ESI) positive: m/z (%) = 484.1312 (100) [$(\mathbf{L1})_2Fe]^+$. MS (ESI) negative: m/z (%) = 195.8104 (80) [$FeCl_4]^-$. IR (ATR) (cm^{-1}): 1610(s) $\upsilon(_{C=N})$.

Synthesis of [bis(2,4-di-tert-butyl-6-{[2-(1H-imidazol-4-yl)-ethylimino]-methyl}-phenol)iron(II)] [triflate] (2): Complex **2** was synthesized using **L2** (0.15 g, 0.45 mmol) and [$Fe(OTF)_2$] (0.16 g, 0.45 mmol) as dark blue crystals. Yield: 0.11 g (22

%). Anal. Calc. for $C_{42}H_{56}F_6N_6O_8FeS_2$: C, 50.10; H, 5.61; N, 8.35; S, 6.37%. Found: C, 49.91; H, 5.79; N, 9.37; S, 4.36%. MS (ESI): m/z (%) = 708.3819 (100) [(**L2**)$_2$Fe]$^+$. IR (ATR) (cm^{-1}): 1599 (s) $\upsilon(_{C=N})$.

Synthesis of (2,4-di-tert-butyl-6-{[2-(1H-imidazol-4-yl)-ethylimino]-methyl}-phenol)iron(III) chloride (3): Complex **3** was synthesized using **L2** (0.16 g, 0.48 mmol) and [$FeCl_2$] (0.06 g, 0.48 mmol) as dark blue crystals. Yield: 0.14 g (67%). Anal. Calc. for $C_{20}H_{28}N_3Cl_2OFe$: C, 53.00; H, 6.23; N, 9.27%. Found: C, 52.92; H, 6.45; N, 9.25%. MS (ESI): m/z (%) = 417 (55) [M-Cl]$^+$, 382 (92) [M-2Cl]$^+$. IR (ATR) (cm^{-1}): 1607 (s) $\upsilon(_{C=N})$.

Synthesis of (2,4-di-tert-butyl-6-{[2-(1H-imidazol-4-yl)-ethylimino]-methyl}-phenol)iron(III) chloride (3): Complex **3** was synthesized using **L2** (0.24 g, 0.72 mmol) and [$FeCl_3$] (0.12 g, 0.72 mmol) as dark blue crystals. Yield: 0.18 g (55%). Anal. Calc. for $C_{20}H_{28}N_3Cl_2OFe.0.125CH_2Cl_2$: C, 52.11; H, 6.14; N, 9.06%. Found: C, 52.13; H, 6.91; N, 9.25%. IR (ATR) (cm^{-1}): 1600 (s) $\upsilon(_{C=N})$.

Synthesis of (2,4-di-tert-butyl-6-{[2-(1H-imidazol-4-yl)-ethylimino]-methyl}-phenol)iron(III) bromide (4): Complex **4** was synthesized using **L2** (0.43 g, 1.31 mmol) and [$FeBr_2$] (0.28 g, 1.31 mmol) as dark blue crystals. Yield: 0.52 g (73%). Anal. Calc. for $C_{20}H_{28}N_3Br_2OFe$: C, 44.31; H, 5.21; N, 7.75%. Found: C, 44.44; H, 5.41; N, 7.70%. MS (ESI): m/z (%) = 463.0747 (5) [M-Br]$^+$, 382.1570 (5) [M-2Br]$^+$, 328.2385 (15) (**L2**). IR (ATR) (cm^{-1}): 1601 (s) $\upsilon(_{C=N})$.

Synthesis of (2,4-di-tert-butyl-6-{[2-(1H-imidazol-4-yl)-ethylimino]-methyl}-phenol)iron(III) iodide (5): Complex **5** was synthesized using **L2** (0.15 g, 0.45 mmol) and [FeI_2] (0.16 g, 0.45 mmol) as dark green powder. Yield: 0.28 g (66%). Anal. Calc. for $C_{20}H_{28}N_3I_2OFe.0.5C_6H_{14}$: C, 40.67; H, 5.19; N, 6.19%. Found: C, 40.04; H, 4.69; N, 6.76%. MS (ESI): m/z (%) = 708.3819 (100) [(**L2**)$_2$Fe]$^+$, 328.2390 (5) [**L2**+H]$^+$. IR (ATR) (cm^{-1}): 1599 (s) $\upsilon_{(C=N)}$.

Synthesis of (4-tert-butyl-2-{[2-(1H-imidazol-4-yl)-ethylimino]-methly}-phenol)iron(III) chloride (6): Complex **6** was synthesized using **L3** (0.53 g, 1.94 mmol) and [$FeCl_2$] (0.25 g, 1.94 mmol) as dark blue powder. Yield: 0.34 g (44%). Anal. Calc. for $C_{16}H_{20}Cl_2FeN_3O.0.25C_6H_{14}$: C, 50.21; H, 5.66; N, 10.04%. Found: C, 50.23; H, 6.18; N, 9.57%. MS (ESI): m/z (%) = 396.2612 (15) (M$^+$), 361.2079(25) (M$^+$-Cl), 272.1757 (100) (ligand). IR (ATR) (cm^{-1}): 1619 (s) $\upsilon_{(C=N)}$.

Synthesis of (2,4-di-tert-butyl-6-{[2-(1H-imidazol-4-yl)-ethylimino]-methyl}-phenol)iron(II) chloride (7): Complex **7** was synthesized using **L2** (0.42 g, 1.27 mmol), [$FeCl_2$] (0.16 g, 1.27 mmol) and Et_3N (0.18 mL, 1.27 mmol) as dark green powder. Yield: 0.35 g (66%). Anal. Calc. for $C_{20}H_{28}N_3ClOFe$: C, 57.50; H, 6.76; N, 10.06%. Found: C, 57.98; H, 6.23; N, 10.10%. MS (ESI): m/z (%) = 708.3811 (100) [(**L2**)$_2$Fe]$^+$, 354.6942 (60) [M/2]$^+$, 382.1606 (10) [M-Cl+H]$^+$, 327.2177 (10) (**L2**). IR (ATR) (cm^{-1}): 1601 (s) $\upsilon_{(C=N)}$.

Supporting Information

Electronic Supporting Information (ESI): This material is available free of charge. Crystallographic data has been deposited with the Cambridge Crystallographic Data Centre with CCDC **998101 (3)**, **998102 (3**, **Figure S2)** and

998103 (4). Copies of this information may be obtained free of charge from the Director, CCDC, 12 Union Road, Cambridge, CB2 1EZ, UK (fax: +44-1223-336063; e-mail: deposit@ccdc.cam.ac.uk or http://www.ccdc.cam.ac.uk.

Acknowledgments

We acknowledge the DST-NRF Centre of Excellence in Catalysis (c*change) and the University of Johannesburg for financial support for this project.

References

1. L. K. Johnson, C. M. Killian, M. Brookhart, *J. Am. Chem. Soc.* **1995**, *117*, 6414-6415.
2. C. M. Killian, L. K. Johnson, M. Brookhart, *Organometallics* **1997**, *16*, 2005-2007.
3. (a) L. K. Johnson, S. Mecking, M. Brookhart, *J. Am. Chem. Soc.* **1996**, *118*, 267-268; (b) S. Mecking, L. K. Johnson, L. Wang, M. Brookhart, *J. Am. Chem. Soc.* **1998**, *120*, 888-899; (c) J. D. Azoulay, G. C. Bazan, G. B. Galland, *Macromolecules* **2010**, *43*, 2794-2800; (d) Z. Guan, P. M. Cotts, E. F. McCord, S. J. McLain, *Science* **1999**, *283*, 2059-2062; (e) T. R. Younkin, E. F. Conor, J. I. Henderson, S. K. Friedrich, R. H. Grubbs, D. A. Bansleban, *Science* **2000**, *287*, 460-462; (f) A. Berkefeld S. Mecking, *Angew. Chem. Int. Ed.* **2008**, *47*, 2538-2542.

4. (a) B. L. Small, M. Brookhart, A. M. A. Bennett, *J. Am. Chem. Soc.* **1998**, *120*, 4049-4050; (b) B. L. Small, M. Brookhart, *J. Am. Chem. Soc.* **1998**, *120*, 7143-7144.

5. (a) V. C. Gibson, C. J. Britovsek, B. S. Kimberley, P. J. Maddox, P. J. Maddox, S. J. McTavish, G. A. Solan, A. J. P. White, D. J. Williams, *Chem. Commun.* **1998**, 849-850. (b) G. J. P. Britovsek, M. Bruce, V. C. Gibson, B. S. Kimberley, P. J. Maddox, S. Mastroianni, S. J. McTavish, C. Redshaw, G. A. Solan, S. Stromberg, A. J. P. White, D. J. Williams, *J. Am. Chem. Soc.* **1999**, *121*, 8728-8740, (c) G. J. P. Britovsek, S. Mastroianni, G. A. Solan, S. P. D. Baugh, C, Redshaw, V. C. Gibson, A. J. P. White, D. J. Williams, M. R. J. Elsegood, *Chem. Eur. J.* **2000**, *6*, 2221-2231.

6. (a) V. C. Gibson, S. K. Spitzmesser, *Chem. Rev.* **2003**, *103*, 283-316; (b) V.C. Gibson, C. Redshaw, G.A. Solan, *Chem. Rev.* **2007**, *107*, 1745-1776.

7. (a) C. Bianchini, G. Giambastiani, L. Luconi, A. Meli, *Coord. Chem. Rev.* **2010**, *254*, 431-455. (b) K. Wang, K. Wedeking, W. Zuo, D. Zhang, W. H. Sun, *J. Organomet. Chem.* **2008**, *693*, 1073-1080. (c) B. L. Small, R. Rios, E. R. Fernandez, M. J. Carney, *Organometallics* **2007**, *26*, 1744-1749. (d) W. -H. Sun, P. Hao, G. Li, S. Zhang, W. Q. Wang, J. J. Yi, M. Asma, N. Tang, *J. Organomet. Chem.* **2007**, *692*, 4506-4518. (e) B. M. Schmiege, M. J. Carney, B. L. Small, D. L. Gerlach, J. A. Halfen, *Dalton Trans.* **2007**, 2547-2562.

8. (a) G. J. P. Britovsek, V. C. Gibson, D. F. Wass, *Angew. Chem. Int. Ed.* **1999**, *38*, 428-447; (b) G. J. P. Britovsek, V. C. Gibson, B. S. Kimberley, S. Mastroianni, C. Redshaw, G. A. Solan, A. J. P. White, D. J. Williams, *Dalton Trans.* **2001**, 1639-1644; (c) J. Ma, C. Feng, S. Wang, K.-Q. Zhao, W.-H.Sun,

C. Redshaw, G. A. Soland, *Inorg. Chem. Front.* **2014**, *1*, 14-34; (d) W. Zhang, W.-H. Sun, C. Redshaw, *Dalton Trans.* **2013**, *42*, 8988-8997.

9. C. Bianchini, G. Giambastiani, I. G. Rios, G. Mantovani, A. Meli, A. M. Segarra, *Coord. Chem. Rev.* **2006**, *250*, 1391-1418.

10. (a) S. Jie, S. Zhang, W.-H. Sun, X. Kuang, T. Liu, J. Guo, *J. Mol. Catal. A: Chem.* **2007**, *269*, 85-96; (b) M. Zhang, P. Hao, W. Zuo, S. Jie, W.-H. Sun, *J. Organomet. Chem.* **2008**, *693*, 483-491; (c) M. Zhang, R. Gao, X. Hao, W.-H. Sun, *J. Organomet. Chem.* **2008**, *693*, 3867-3877; (d) C. Bianchini, G. Mantovani, A. Meli, F. Migliacci, F. Laschi, *Organometallics* **2003**, *22*, 2545-2547; (e) L. Xiao, R. Gao, M. Zhang, Y. Li, X. Cao, W.-H. Sun, *Organometallics* **2009**, *28*, 2225-2233.

11. (a) S. A. Svejda, L. K. Johnson, M. Brookhart, *J. Am. Chem. Soc.* **1999**, *121*, 10634-10635; (b) D. J. Tempel, L. K. Johnson, R. L. Huff, P. S. White, M. Brookhart, *J. Am. Chem. Soc.* **2000**, *122*, 6686-6700.

12. G. J. P. Britovsek, G. K. B. Clentsmith, V. C. Gibson, D. M. L. Goodgame, S. J. McTavish, Q. Pankhurst, *Catal. Commun.* **2002**, *3*, 207-211.

13. (a) A. S. Ionkin, W. J. Marshall, D. J. Adelman, B. Bobik Fones, B. M. Fish, M. F. Schiffhauer, *Organometallics* **2006**, *25*, 2978-2992. (b) C. Görl, H. G. Alt, *J. Organomet. Chem.* **2007**, *692*, 4580-4592. (c) A. S. Ionkin, W. J. Marshall, D. J. Adelman, B. Bobik Fones, B. M. Fish, M. F. Schiffhauer, P. D. Soper, R. L. Waterland, R. E. Spence, T. Xie, *J. Polym. Sci., A: Polym. Chem.* **2008**, *46*, 585-611.

14. (a) P. Hao, Y. J. Chen, T. P. F. Xiao, W.-H. Sun, *J. Organomet. Chem.* **2010**, *695*, 90-95; (b) A. S. Ionkin, W. J. Marshall, D. J. Adelman, A. L. Shoe, R. E.

Spence, T. Y. Xie, *J. Polym. Sci., Part A: Polym. Chem.* **2006**, *44*, 2615-2635; (c) A. S. Ionkin, W. J. Marshall, D. J. Adelman, B. B. Fones, B. M. Fish, M. F. Schiffhauer, *Organometallics* **2006**, *25*, 2978-2992.

15. (a) T. Matsugi, T. Fujita, *Chem. Soc. Rev.* **2008**, *37*, 1264-1277; (b) Y. Nakayama, J. Saito, H. Bando, T. Fujita, *Chem. Eur. J.* **2006**, *12*, 7546-7556; (c) H. Terao, S.-I. Ishii, J. Saito, S. Matsuura, M. Mitani, N. Nagai, H. Tanaka, T. Fujita, *Macromolecules* **2006**, *39*, 8584-8593; (d) A. F. Mason, G. W. Coates, *J. Am. Chem. Soc.* **2004**, *126*, 10798-10799; (e) G. Paolucci, A. Zanella, L. Sperni, V. Bertolasi, M. Mazzeo, C. Pellecchia, *J. Mol. Catal. A: Chem.* **2006**, *258*, 275-283.
16. (a) R. K. O'Reilly, V. C. Gibson, A. J. P. White, D. J. Williams, *J. Am. Chem. Soc.* **2003**, *125*, 8450-8451; (b) M. S. Shongwe, B. A. Al-Rashdi, H. Adams, M. J. Morris, M. Mikuriya, G. R. Hearne, *Inorg. Chem.* **2007**, *46*, 9558-9568.
17. (a) M. Zhang, W. Zhang, T. Xiao, J.-F. Xiang, X. Hao, W.-H. Sun, *J. Mol. Catal. A: Chem.* **2010**, *320*, 92-96; (b) W.-H. Sun, X. Tang, T. Gao, B. Wu, W. Zhang, H. Ma, *Organometallics* **2004**, *23*, 5037-5047.
18. (a) N. F. Curtis, *J. Chem. Soc.* **1964**, 2644-2650; (b) N. F. Curtis, D. F. Cook, *Chem. Commun. (London),* **1967**, 962-963; (c) G. C. Dobinson, R. Mason, D. R. Russell, *Chem. Commun. (London),* **1967**, 62-63; (d) B. N. Figgis, J. Lewis, *Prog. Inorg. Chem.* **1964**, *6*, 197.
19. A. S. Abu-Surrah, K. Lappalainen, U. Piironen, P. Lehmus, T. Repo, M. Leskelä, *J. Organomet. Chem.* **2002**, *648*, 55-61.

20. (a) Z. Zhang, J. Zou, N. Cui, Y. Ke, Y. Hu, *J. Mol. Catal. A: Chem.* **2004**, *219*, 249-254; (b) R.-F. Chen, C.-T. Qian, J. Sun, *Chin. J. Chem.* **2001**, *19*, 866-869.

21. A. W. Addison, T. N. Rao, J. Reedijk, J. van Rijn, G. C. Verschoor, *J. Chem. Soc. Dalton Trans.* **1984**, 1349-1356.

22. W.-H. Sun, P. Hao, S. Zhang, Q. Shi, W. Zuo, X. Tang, *Organometallics* **2007**, *26*, 2720-2734.

23. (a) R. Herchel, Z. Šindelář, Z. Trávníček, R. Zbořil, J. Vančo, *Dalton Trans.* **2009**, 9870-9880; (b) B. Djukic, P. K. Poddutoori, P. A. Dube, T. Seda, H. A. Jenkins, M. T. Lemaire, *Inorg. Chem.* **2009**, *48*, 6109-6116.

24. N. Moliner, J. A. Real, M. C. Muñoz, R. Martínez-Mañez, J. M. C. Juan, *J. Chem. Soc., Dalton Trans.* **1999**, 1375-1379.

25. (a) H. H. Wickman, A. M. Trozzolo, H. J. Williams, G. W. Hull, F. R. Merritt, *Phys. Rev.* **1967**, *155*, 563-; (b) H. H. Wickman, A. M. Trozzolo, *Inorg. Chem.* **1968**, *7*, 63-68; (c) L. M. Epstein, D. K. Straub, *Inorg. Chem.* **1969**, *8*, 560-562.

26. (a) Y. Hosokoshi, K. Katoh, Y. Nakazawa, H. Nakano, K. Inoue, *J. Am. Chem. Soc.* **2001**, *123*, 7921-7922; (b) C. Mathonière, C. J. Nuttall, S. G. Carling, P. Day, *Inorg. Chem.* **1996**, *35*, 1201-1206.

27. (a) R. Hernández-Molina, A. Mederos, S. Dominguez, P. Gili, C. Ruiz-Pérez, A. Castiñeiras, X. Solans, F. Lloret, J. A. Real, *Inorg. Chem.* **1998**, *37*, 5102-5108; (b) B. Djukic, P. A. Dube, F. Razavi, T. Seda, H. A. Jenkins, J. F. Britten, M. T. Lemaire, *Inorg. Chem.* **2009**, *48*, 699-707.

28. P. Gütlich, J. Ensling, *Mössbauer spectroscopy, in Inorganic Electronic Structure and Spectroscopy.* Vol. I. Methodology, E. I. Solomon and A. B. P. Lever (Eds.), Wiley-Interscience, New York, **1999**.

29. (a) A. N. Buckley, G. V. H. Wilson, K. S. Murray, *Solid State Commun.* **1969**, *7*, 471-474; (b) W. M. Reiff, G. J. Long, W. A. Baker, Jr., *J. Am. Chem. Soc.* **1968**, *90*, 6347-6351.

30. N. N. Greenwood, T. C. Gibb, in *Mössbauer Spectroscopy*, Chapman and Hall Ltd, London, **1971**.

31. (a) F. Speiser, P. Braunstein, L. Saussine, *Acc. Chem. Res.* **2005**, *38*, 784-793; (b) C. E. Anderson, A. S. Batsanov, P. W. Dyer, J. Fawcett, J. A. K. Howard, *Dalton Trans.* **2006**, 5362-5378; (c) E. Y.-X. Chen, T. J. Marks, *Chem. Rev.* **2000**, *100*, 1391-1434. (d) M. Sauthier, F. Leca, R. De Souza, K. Bernardo-Gusmaõ, L. F. T. Queiroz, L. Toupet, R. Reáu, *New J. Chem*. **2002**, *26*, 630-635.

32. A. Boudier, P.-A. R. Breuil, L. Magna, C. Rangheard, J. Ponthus, H. Olivier-Bourbigou, P. Braunstein, *Organometallics* **2011**, *30*, 2640-2642.

33. (a) W.-H. Sun, P. Hao, S. Zhang, Q. Shi, W. Zuo, X. Tang, X. Lu, *Organometallics* **2007**, *26*, 2720-2734; (b) C. Görl, T. Englmann, H. G. Alt, *Appl. Catal. A: Gen.* **2011**, *403*, 25-35.

34. S. O. Ojwach, I. A. Guzei, L. L. Benade, S. F. Mapolie, J. Darkwa, *Organometallics* **2009**, *28*, 2127-2133.

35. A. Budhai, B. Omondi, S. O. Ojwach, C. Obuah, E. Y. Osei-Twum, J. Darkwa, *Catal. Sci. Technol.* **2013**, *3*, 3130-3135.

36. C. Obuah, B. Omondi, K. Nozaki, J. Darkwa, *J. Mol. Catal. A: Chem.* **2014**, *382*, 31-40.

37. P. J. Flory, *J. Am. Chem. Soc.* **1940**, *62*, 1561-1565; (b) G. V. Z. Schulz, *Phys. Chem. Abt. B* **1935**, *30*, 379-398; (c) G. V. Z. Schulz, *Phys. Chem. Abt. B* **1939**, *43*, 25-46.

38. (a) T. Usami, S. Takayama, *Macromolecules* **1984**, *17*, 1756-1761; (b) G. B. Galland, R. F. de Souza, R. S. Mauler, F. F. Nunes, *Macromolecules* **1999**, *32*, 1620-1625.

39. (a) S. D. Wilson, H.-Y. Huang, *J. Chin. Chem. Soc.* **1936**, *4*, 142. (b) W. L. Mendelson, C. B. Spainhour, S. S. Jones, B. L. Lam, K. L. Wert, *Tetrahedron Lett.* **1980**, *21*, 1393-1396; (c) W. F. Beckert, J. U., Jr. Lowe, *J. Org. Chem.* **1967**, *32*, 582-584; (d) J. S. Han, W. C. Lim, B. R. Yoo, J. -I. Jin, I. N. Jung, *Organometallics* **2002**, *21*, 3803-3809.

40. (a) R. Walsh, D. H. Morgan, A. Bollmann, J. T. Dixon, *Appl. Catal. A: Gen.* **2006**, *306*, 184-191. (b) S. Kuhlmann, J. T. Dixon, M. Haumann, D. H. Morgan, J. Ofili, O. Spuhl, N. Taccardi, P. Wasserscheid, *Adv. Synth. Catal.* **2006**, *348*, 1200-1206.

41. J. Skupinska, *Chem. Rev.* **1991**, *91*, 613-648.

42. L. Casella, M. Gullotti, A. Pintar, L. Messori, A. Rockenbauer, M. Györ, *Inorg. Chem.* **1987**, *26*, 1031-1038.

43. S. Boltina, M. Yankey, I. A. Guzei, L. C. Spencer, S. O. Ojwach, J. Darkwa, *S. Afr. J. Chem.* **2012**, *65*, 75-83.

44. *Bruker-AXS. (***2007***) APEX2, SADABS, and SAINT Software Reference Manuals. Bruker-AXS,* Madison, Wisconsin, USA.

45. O. V. Dolomanov, L. J. Bourhis, R. J. Gildea, J. A. K. Howard, H. Puschmann, *OLEX2: A complete structure solution, refinement and analysis program*. *J. Appl. Cryst.* **2009**, *42*, 339-341.

(Salicyladimine)iron(III) pre-catalysts, from iron(II) precursors, form catalysts for ethylene oligomerisation, polymerisation and alkylation of aromatic solvents by the ethylene oligomers.